

Structural analysis of the Barrô Romanesque Church

Análise estrutural da Igreja Românica de Barrô

Daniel V. Oliveira
Bledian Nela
Eduarda Vila-Chã
Nilma Muñiz
Pablo Bañasco
Pratik N. Gajjar

Abstract

Built on the left bank of the Douro River, the Romanesque Church of Barrô was founded in the 12th century. This church underwent many changes during its service years. The damage level and mechanical properties of the structure were evaluated through NDT. From these tests, it was possible to evaluate the structural properties with a comfortable reliable confidence level and form a detailed damage map. With the purpose of determining the cause of the damages and suggesting proper conservation, a numerical nonlinear analysis was performed in order to evaluate the vertical load-carrying capacity of the structure. Lateral pushover analysis was also performed in both directions to observe the seismic performance of the structure. Finally, preventive measures are recommended, together with a detailed monitoring plan to increase the confidence and knowledge level of the structure.

Resumo

Construída na margem esquerda do Rio Douro, a Igreja Românica de Barrô foi fundada no século XII. Esta igreja sofreu inúmeras alterações ao longo do tempo. O nível de dano instalado e as propriedades mecânicas da estrutura foram avaliados através de ensaios NDT. A partir destes testes, foi possível avaliar as propriedades estruturais com um nível de confiança elevado e obter um mapa de danos detalhado. Com o objetivo de determinar a causa dos danos e propor uma conservação adequada, foi realizada uma análise numérica não linear para avaliar a capacidade de carga vertical da estrutura. Foi realizada também a análise *pushover* em ambas as direções para conhecer o desempenho sísmico da estrutura. Por fim, são recomendadas medidas preventivas, juntamente com um plano de monitorização detalhado para aumentar a confiança e o nível de conhecimento da estrutura.

Keywords: Historical structure / Masonry / Monitoring / Non-destructive testing / Structural analysis

Palavras-chave: Estrutura histórica / Alvenaria / Monitorização / Ensaios não-destrutivos / Análise estrutural

Daniel V. Oliveira

University of Minho, ISISE
Guimarães – Portugal
danvco@civil.uminho.pt

Bledian Nela

Sapienza University of Rome
Rome – Italy
bledian.nela@uniroma1.it

Eduarda Vila-Chã

University of Minho
Guimarães – Portugal
eduarda.vila.cha26@gmail.com

Nilma Muñiz

University of Minho
Guimarães – Portugal
nilma.muniz@upr.edu

Pablo Bañasco

University of Minho
Guimarães – Portugal
plbs1988@gmail.com

Pratik N. Gajjar

University of Minho, ISISE
Guimarães – Portugal
pratik.gajjar@civil.uminho.pt

Aviso legal

As opiniões manifestadas na Revista Portuguesa de Engenharia de Estruturas são da exclusiva responsabilidade dos seus autores.

Legal notice

The views expressed in the Portuguese Journal of Structural Engineering are the sole responsibility of the authors.

OLIVEIRA, D. [et al.] – Structural analysis of the Barrô Romanesque Church. **Revista Portuguesa de Engenharia de Estruturas**. Ed. LNEC. Série III. n.º 17. ISSN 2183-8488. (novembro 2021) 61-70.

1 Introduction

The Barrô Church, also known as Saint Mary Church, an important architectural heritage of Romanesque, stands along the Douro river valley, in the heart of the North of Portugal. This church unfolds a late Romanesque style with some Baroque and Gothic features, which was introduced in Portugal in the late 11th century and prevailed until the end of the 13th. The development of this architectural style occurred due to Christian reconquer along Europe. The expansion of the Romanesque architecture in Portugal occurred at the same time D. Afonso Henriques (First King of Portugal) assumed the Government in 1128 and started to conquer territories towards the South. The materials used were those available in each region, which, in the case of northern Portugal, was granite.

The Church shows historical data of its existence since the 12th century, but remaining traces suggest that its construction began in the first half of the 13th century. Since the construction, it has suffered several interventions over time. In particular, a bell tower was built at the end of the 17th century and then reconstructed in 1890. Additional important works were carried out in the 20th century, where “*Sala das Almas*” was demolished and major problems with water infiltration were tackled afterward by changing the roof tiles and introducing gutters and drainage channels in 1966. The present church consists of a Chancel, Main Nave, Sacristy, and the Bell Tower, which can be seen in Figure 1a. The historical timeline can be observed in the form of a stratigraphic model in Figure 1b. The Church of Barrô is classified as a national monument since 1922 and is part of the Portuguese Romanesque Route (Monument #31) since 2010.

Mainland Portugal is located on the West part of the Eurasian plate, in the vicinity of the African Plate. Therefore, the seismic activity in the area is an important aspect to have into consideration. The most relevant events during the lifetime of the Barrô Church can be seen in Table 1. From historical data, it is noted that the Lisbon earthquake in 1755 affected the church by collapsing partially the cross and damaging the belfry, which was rebuilt in the 20th century.

Table 1 Relevant historical seismic activity [1]

Location	Date	Magnitude	Distance to Barrô
Lisboa	November 1, 1755	8.5	285 km
Porto	April 13, 1783	5.00 ± 0.50	60 km
Braga	May 2, 1793	4.46 ± 0.50	65 km
Moncorvo	March 19, 1858	5.36 ± 0.58	45 km

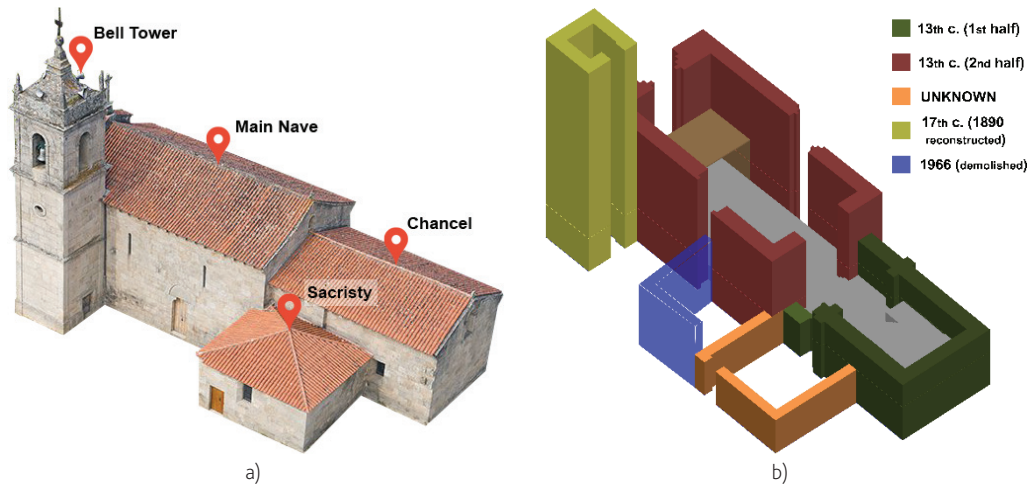


Figure 1 Church of Barrô: a) main components; b) stratigraphic model

2 Geometrical survey

In the absence of any drawings of the church, a detailed geometrical survey was carried out. The geometrical survey is a basic requirement for any assessment of cultural heritage as it presents the foundation to plan and manages all other processes. The detailed geometrical survey was conducted in the traditional methodology and external photogrammetry of the church was utilized for the 3-dimensional

geometry of the building that was used in the later steps. The geometrical survey followed the usual traditional techniques of initially sketching the building and taking precise measurements to be followed by CAD drawings. The final drawings produced are a total of twelve precise and deformation-inclusive drawings of base plans, facades, and sections. Photogrammetry was carried out to form a 3D model of the building and to obtain a spatial idea of the deformations and damage. An example of the drawings and the photogrammetric model are shown in Figure 2. As merely informative, the main façade is 13 m long and the tower is around 21 m high.

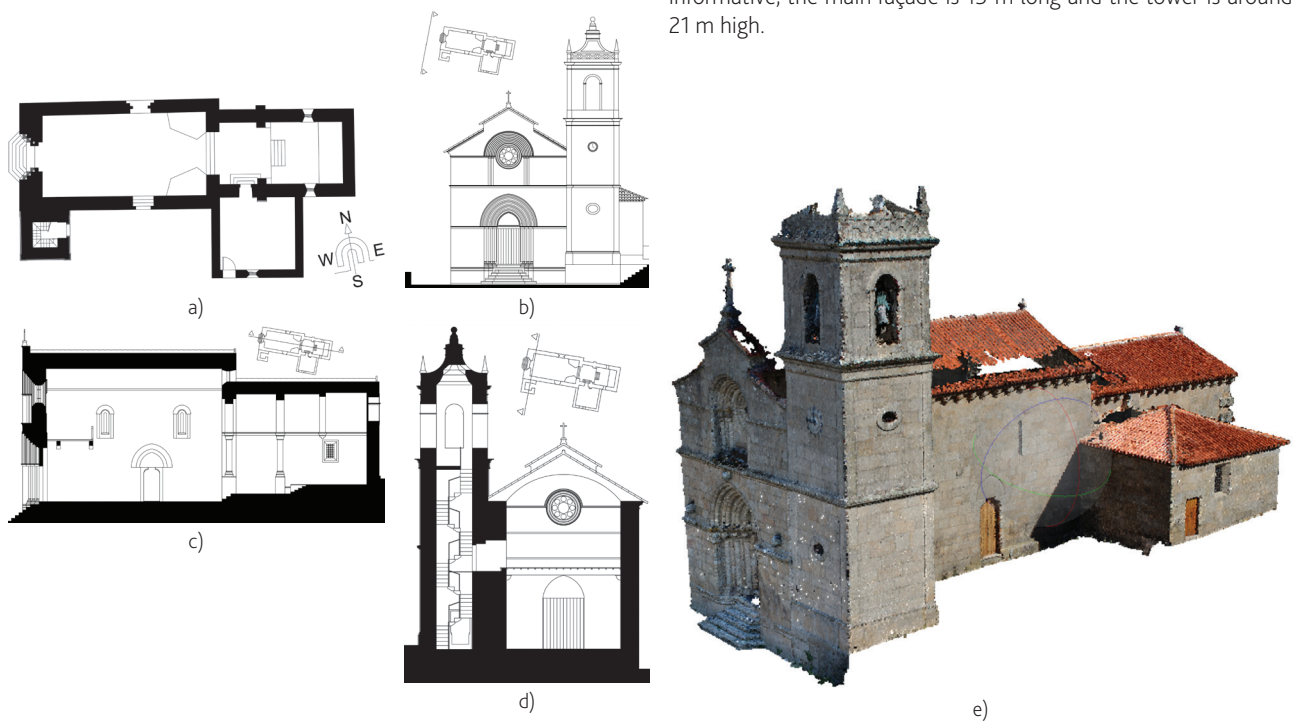


Figure 2 Geometry of the church: a) plan; b) elevation; c) section along east-west; d) section along north-south; e) 3D photogrammetric model

3 Damage identification

The state of Barrô Church was evaluated through a visual inspection to identify actual damages. The exterior and interior were evaluated, and the damages were classified according to ICOMOS Guidelines [2] and following the HeritageCare inspection procedure [3]. The damages were classified into five principal categories: cracks and deformation, detachment, material loss, discoloration and deposit, and biological colonization. This method is considered one of the most effective methods to qualify the real state of the structure.

3.1 Damage identification of the exterior

The exterior of the Church showed disintegration of the granite

stone with signs of detachment of single grains or aggregates of grains. Scaling detachment was observed in localized parts. This is an effect of decay that can be related to the erosion of stones due to salt crystallization. The exterior of the Church shows other damages due to erosion, including loss of matrix and rounding of the edges close to the joints. There are also missing parts of the façade elements. The façades of Barrô Church have several cracks that can be classified as fractures. Especially in the West façade, significant cracks were observed in the wall above the choir. The West façade also shows a black crust. Around the Church, several types of biological colonization were observed, including plants, algae, and lichens. Biofilm was also observed, especially in the North Façade. Figure 3 shows the damage maps drawn on top of the Photoscan model mapped according to [2].

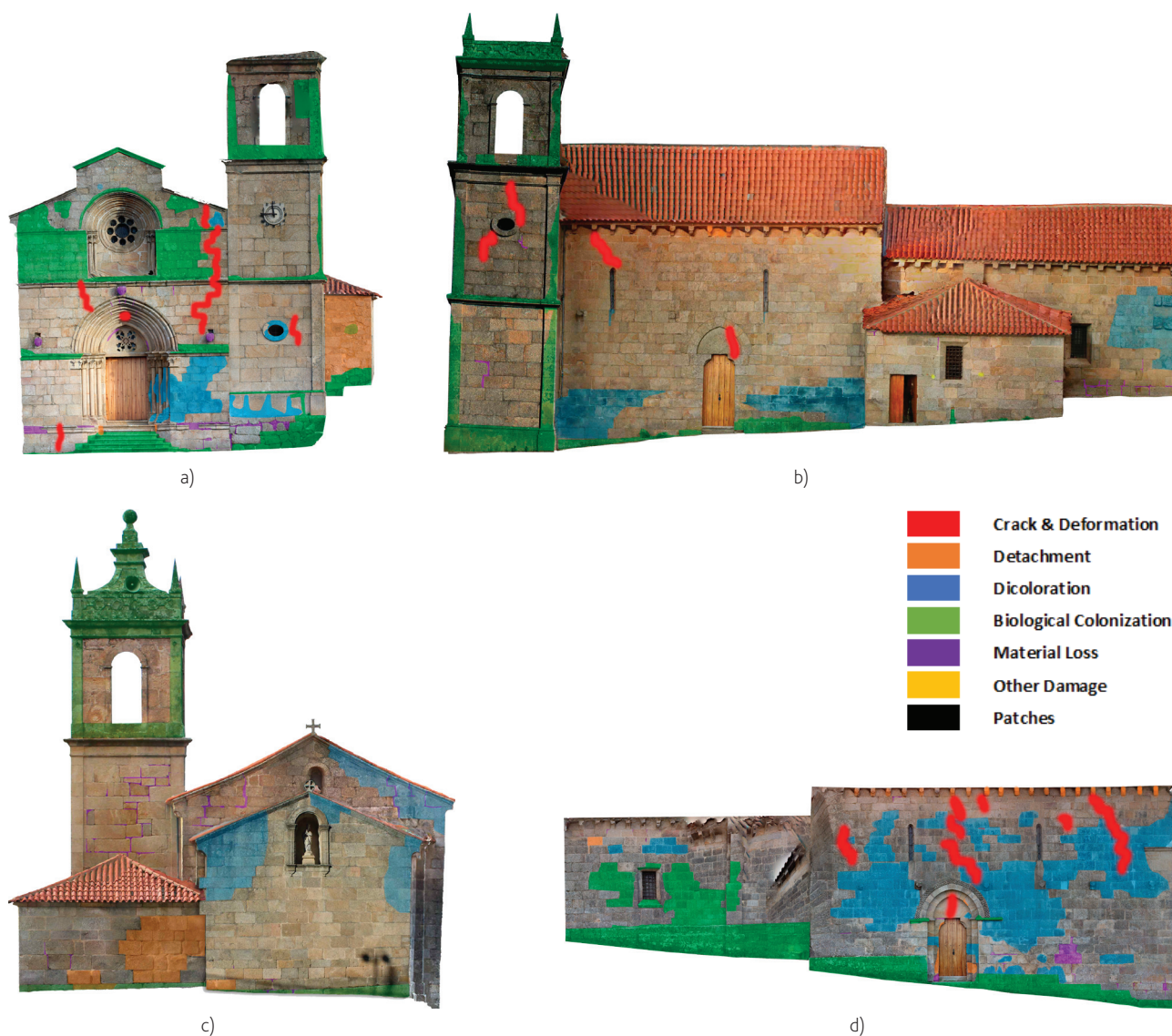
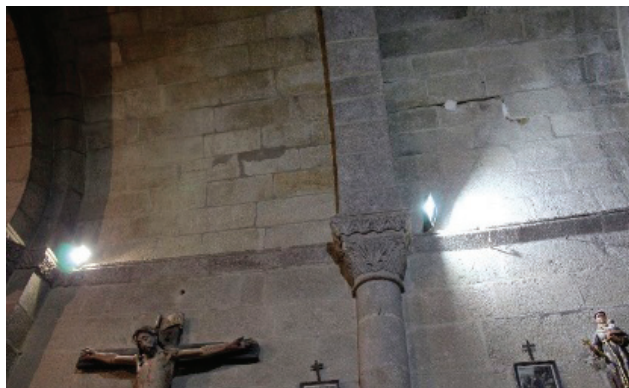


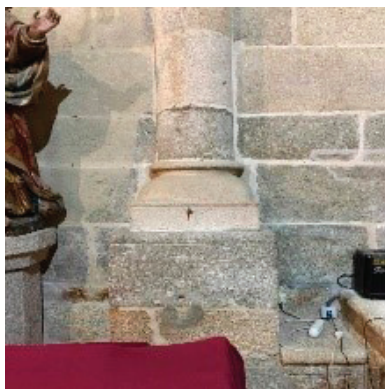
Figure 3 Damage maps: a) west facade; b) south façade; c) east façade; d) north façade

3.2 Damage identification of the interior

The interior of the Church shows signs of cracking. The most significant crack is visible in the vault of the main chapel. The North façade wall of the Church has signs of deformation, which was observed clearly from the interior of the Church since the wall and one of the columns of the Main Chapel are exhibiting concave deformation. The interior of the Church shows signs of patina and staining due to moisture. Figure 4 shows the damages described, respectively from left to right.



a)



b)



c)

Figure 4 Interior damage: a) crack in the vault; b) deformation of the column; c) patina

4 Non-destructive testing

A series of non-destructive tests were performed in the church to obtain the state of the damage and the relevant mechanical parameters for the numerical model. After a careful and detailed visual inspection, the tests were conducted based on the availability of the testing equipment and permission from the owner.

4.1 Masonry Quality Index (MQI)

The initial approach for the assessment and categorization of the masonry was done utilizing the Masonry Quality Index (MQI) proposed by [4], which through the visual and qualitative inspection quantifies the mechanical parameters. The MQI was computed for the 4 stages of construction of the church, which represent different periods in the historical timeline of the church. The assessment was done namely for the Chancel, the Main Nave, the Bell Tower, and the Sacristy. Assessing the similar pattern of masonry (in terms of size and shape), only one most representative element per construction stage was considered. The results of MQI are shown for the four stages of construction in Table 2, where upper bound and lower bound properties are marked with UB and LB, respectively. It can be seen from these results that the later construction stages present better masonry mechanical properties compared to the older ones, as it can be compared also from the damage identification.

4.2 Thermography

Temperature measurements were carried out on different parts of the church to identify superficial deterioration, hidden damage, moisture, and geometry definition of hidden elements. Utilizing a thermal camera several measurements were performed in the church. Figure 5 presents the locations of these measurements together with the location of the other tests performed. Some of the most representative examples of thermal pictures are shown in Figure 6, which are names respectively to their location in Figure 5.

Tabela 2 Mechanical properties obtained from MQI for masonry

	Compressive strength f_c [MPa]		Young's Modulus E [GPa]		Shear Strength τ_0 [MPa]	
	LB	UB	LB	UB	LB	UB
Chancel	4.0	6.0	1.70	2.40	0.080	0.110
Nave	8.5	12.2	3.10	4.20	0.165	0.220
Sacristy	2.0	3.2	0.95	1.40	0.037	0.057
Tower	8.5	12.2	3.10	4.20	0.165	0.220

From TRM_7, it can be observed that on the left side there is a clear separation of the arch above the door to the stone filling underneath, not clearly visible to the naked eye. Additionally, from TRM_11 another distinct separation between the sculpture stand and the rest of the wall can be seen. TRM_15 shows material differences between the altar and the stone vault, which has a clear

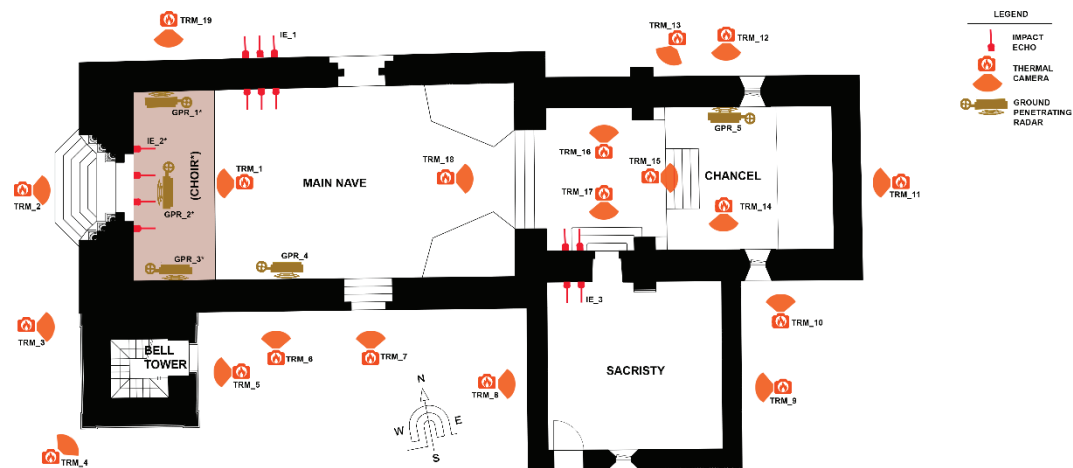


Figure 5 Non-destructive test locations (*for the tests in the Choir level)

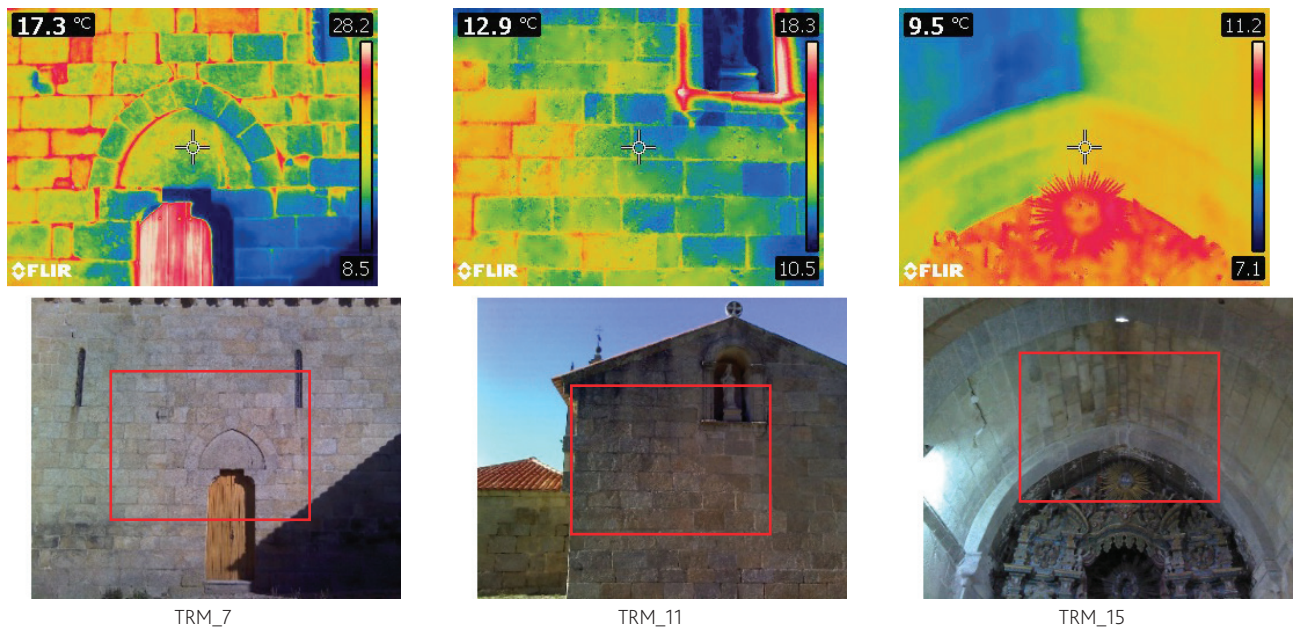


Figure 6 Thermal camera pictures (top) and the part they represent (bottom)

thermal separation line at the apex. This separation comes from the orientation of the church where the left side (of this picture) is the northern side whereas the right side is the southern side, which at the time of measurement was constantly in contact with the sun.

4.3 Ground Penetrating Radar (GPR)

Ground-penetrating radar was utilized in order to understand the inner constitution of the walls, identify any presence of damage and measure the thickness of the walls and the vault. The measurements were carried out with an 800 MHz antenna and the locations are shown in Figure 5. The GPR_1 radargram (Figure 7a) shows an internal view of the crack in that part of the wall. Patterns of hyperbolas show a specific trend rather than being random as

they would be on a normal wall and this explains the cracks as the consequence of detachment. From the GPR_2 radargram (Figure 7b) one can observe a difference in amplitude from the rest of the wall that is at the inner layer and the external interior masonry, which indicates a thicker separation between the layers and thus explaining the out-of-plane deformation perceived. On the southern wall in the choir level (GPR_3) a clear separation between the nave wall and the tower wall can be seen from the radargram in Figure 7c.

The radargrams for the walls (GPR_4 and GPR_5) show that the walls are composed of three-leaf walls, the inner layer is very regular and they contain a large number of interlocking stones (Figure 7d and Figure 7e). Lastly, from the measurement at the starting of the vault (GPR_5), it is found out that the thickness at its start is around 50 cm, which can be seen from Figure 7f.

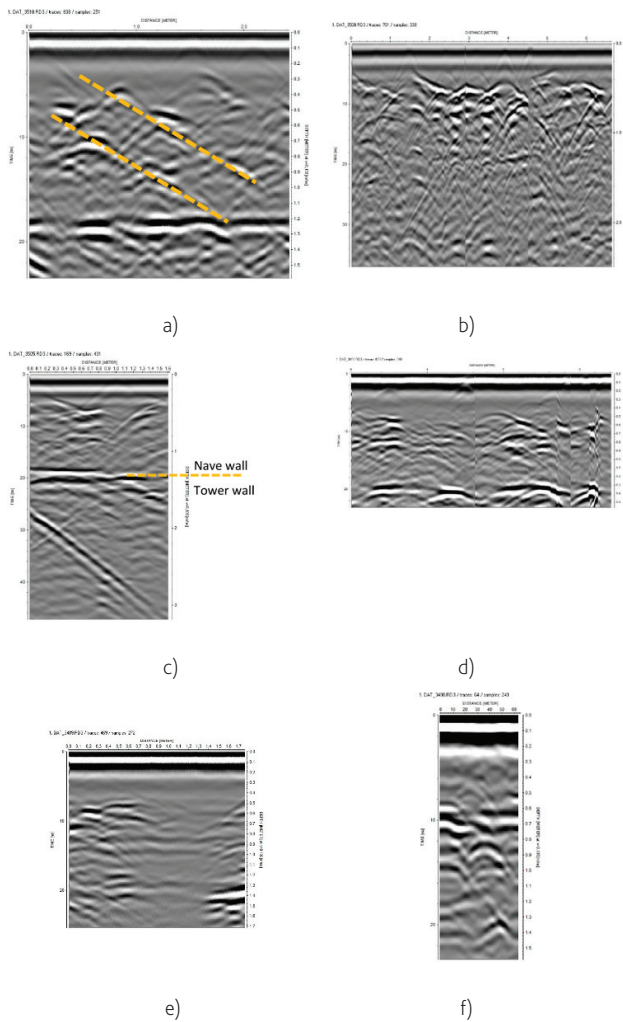


Figure 7 Radargrams at: a) GPR_1 northern wall choir level; b) GPR_2 western façade wall choir level; c) GPR_3 southern nave-tower wall interface choir level; d) GPR_4 southern wall; e) GPR_5 northern wall; f) GPR_5 beginning of the vault

4.4 Impact-echo test

The elastic wave method impact-echo was performed in 3 locations as shown above in Figure 5, where IE_1 and IE_3 with the direct method and IE_2 with the indirect method. IE_1 was carried out in 9 points with a layout of 3 by 3 points each separated 50 cm from each other. The elastic modulus is correlated with the velocities utilizing the formulations for P and R waves and a Poisson's ratio of 0.2 and a common density for stones of about 2.2 ton/m³. Similarly, for the test IE_3, 6 points with a layout of 2 by 3 each separated by 50 cm from each other were tested. The correlation between the velocities and elastic modulus for tests IE_1 and IE_3 is shown in Figure 8. A mean elastic modulus value comes up to be around 2.0 GPa with slight deviations in some points of IE_1 and only one

point of deviation in IE_3, which may be due to the presence of interlocking stones.

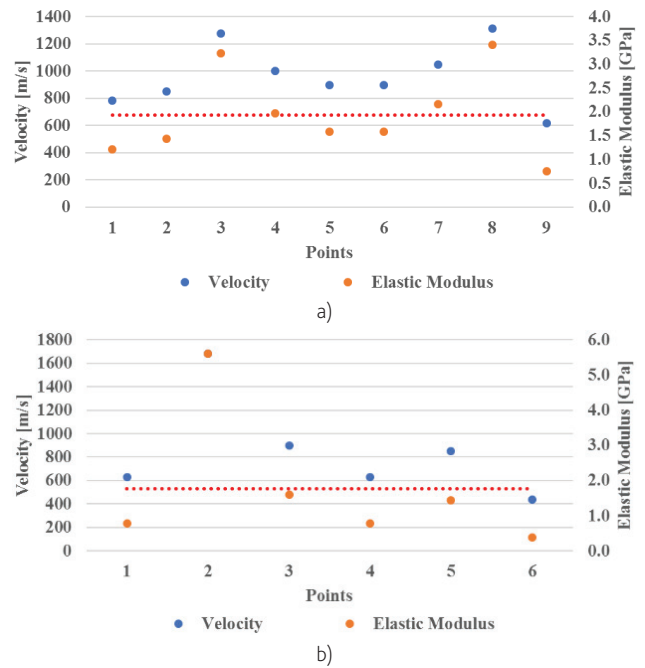


Figure 8 Correlation between velocity and the elastic modulus in: a) northern wall IE_1; b) southern wall IE_3

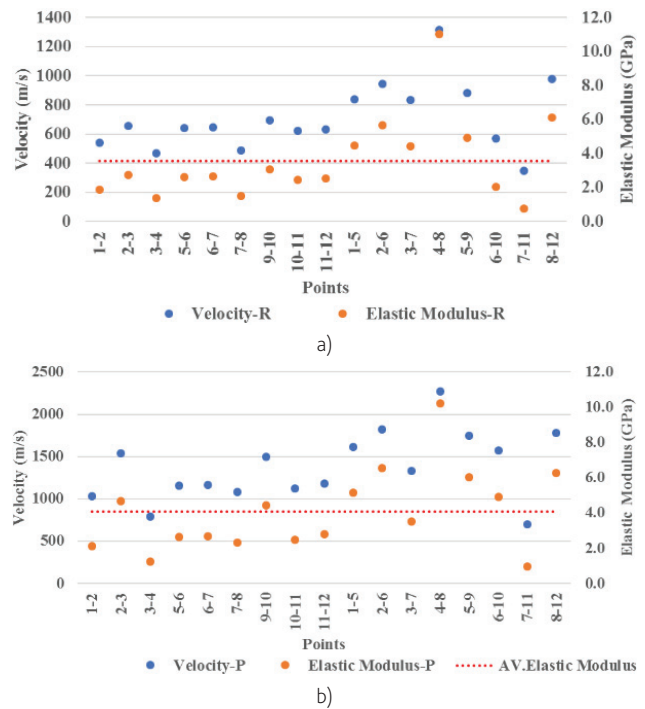


Figure 9 Correlation between velocity and the elastic modulus: a) R-waves; b) P-waves

In contrast, 12 points were measured in IE_2 (choir level) with a layout of 4 by 3 separated by 50 cm in the vertical direction and 100 cm in the horizontal direction (shown in Figure 9). The mean elastic modulus from the P-wave and R-wave measurements is around 4.0 GPa with a deviation at point 4-8.

4.5 Rebound hammer test

The rebound hammer test provides a superficial measurement of the hardness of materials. In the case of stone masonry with dry joints the rebound hammer gives only qualitative measurements of surface hardness as to be compared relatively between different locations in the church (outside “EXT” and inside “INT”). This comparison is done with the sole purpose of identifying the weaker spots of the masonry. The rebound values from this test are shown in the form of a table and visually classified represented by distinctive colors in Figure 10.

	Min	Max	Avg	SD	CoV
Nave_INT	22	50	32.5	5.7	18%
Nave_EXT	10	50	31.1	7.8	25%
Chancel_INT	14	45	30.7	6.7	22%
Chancel_EXT	12	60	27.6	7.5	27%
Sacristy_EXT	12	52	28.4	8.1	28%
Tower_INT	15	41	28.4	6.8	24%

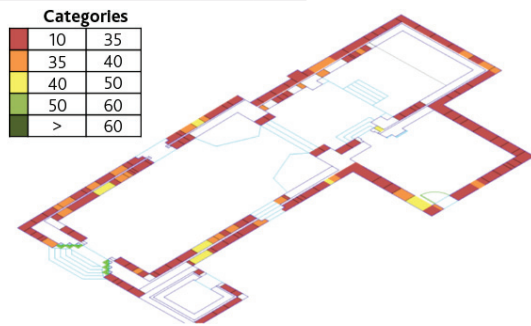


Figure 10 Results from the rebound hammer in the form of a table (left) and visual classification (right)

5 Numerical model and structural assessment

A numerical model was built in commercial FEA DIANA software [5], using solid structural elements to observe the behaviour of the structure in nonlinear pushover cases. The assumptions, boundary conditions, loads, and material properties are mentioned in the following sections.

5.1 Assumptions

Due to the complex geometry and the present condition of the church, some assumptions were made in the numerical model, such

as, the roofing system of the main nave was not considered in the FEA model, only the equivalent loading for the roofing system was considered [5]. A constant thickness of 500 mm was considered for the vault due to some geometric unknowns; this thickness was considered based on the findings from the GPR test. A lightweight filling of 1800 kg/m³ was considered at the top of the vault. Due to the sloping nature of the resting ground, the base of the walls was considered in a continuous stepped way as it was witnessed on site. Considering the geometry and these assumptions, the FEA model considered for further analysis is shown in Figure 11.

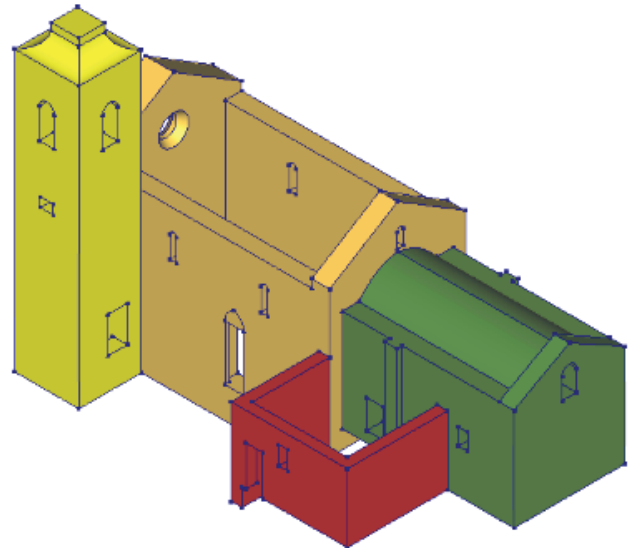


Figure 11 3D visualization of the FEA model

5.2 Material properties

The definition of mechanical properties is a crucial task in the modeling phase since material properties are rarely available in heritage structures. The most reliable source of such properties is non-destructive tests that most of the time, provide qualitative information that can be converted into mechanical properties through correlations available in the literature. From the NDT tests performed, correlations and suggestions available in the literature [6], [7], [8], and [9] the following material properties presented in Table 3 were considered for the analyses.

Table 3 Material mechanical properties

Properties	Main Nave / Bell Tower / Sacristy	Main Chapel
Young's modules [GPa]	4.0	3.0
Compressive strength [MPa]	5.7	4.3
Compressive fracture energy [N/mm]	9.1	6.9
Tensile strength [MPa]	0.3	0.2
Tensile fracture energy [N/mm]	0.03	0.02

5.3 Boundary conditions and loads

As discussed earlier, the structure is located on sloping ground, with rocky strata. From the site inspection, stepped continuous footings along the wall were observed. Also, from the visual inspection, it was observed that the north wall of the main chapel is bulging outside with a degree varying from 4 to 1 from east to west direction. The cause of this observation was traced to the actions done by either a seismic activity or due to differential settlements of the structure. For that reason, two different types of support systems were applied to observe the behavior of that wall in the linear elastic analysis. The first support system was composed of hinge supports applied to the foundation level surfaces and in the other model, the support consisted of subgrade elasticity at the foundation level. The observations made from the linear elastic analysis of both modeled to the same results for the bulging of the northern wall. As no difference between the results was found, it was decided to use hinge support for surfaces for the nonlinear analysis.

For static gravity loads, the self-weight of given material was considered at a global level and for the roofing at the main nave, and the structure adjoining to the main chapel, equivalent loads were applied instead of the modeling of the roofing structure. For the filling at the main chapel vault, a lightweight filling of 1800 kg/m³ was applied as projected loads.

5.4 Analysis of the load carrying capacity

In order to observe the present vertical load-bearing capacity of the structure, and derive the vertical load safety factor, a nonlinear pushdown analysis was performed. In this analysis, gravity forces were applied in increasing steps and analysis was deemed to be completed when major damage at the junction of wall and vault was observed. The total weight of the structure for the gravity loading was calculated as 2224 tons. Figure 12a shows the vertical load factor normalized concerning the total deadweight of the structure plotted against the vertical displacement at the center of the vault and tower top. Figure 12b shows the crack distribution observed for this analysis at peak load (load factor of 3.79).

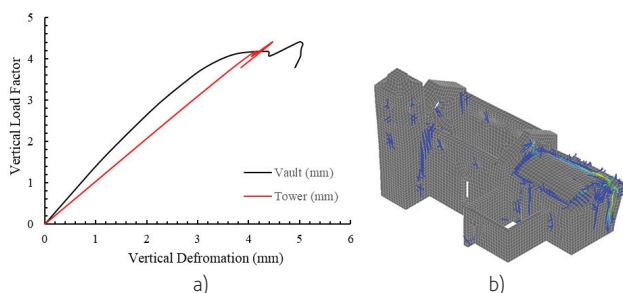


Figure 12 Results of pushdown analysis: a) capacity curve; b) crack distribution

5.5 Pushover analysis

The pushover analysis was performed applying an equivalent acceleration in the North-South and East-West directions, with

forces proportional to the mass. For the pushover analysis, gravity forces were initially applied, and a horizontal acceleration was imposed with appropriate load steps. The analysis was performed with the modified Newton-Raphson method. This was done to solve the non-linear equilibrium equations and find convergence based on energy balance. After performing the pushover analysis, displacement vs load factor was computed for the extreme points of the structure. From the lateral pushover in the east-west direction, the lateral capacity was found to be 0.15 g (Figure 13a) and damage at the peak load (0.21 g) in terms of crack distribution is shown in Figure 13b.

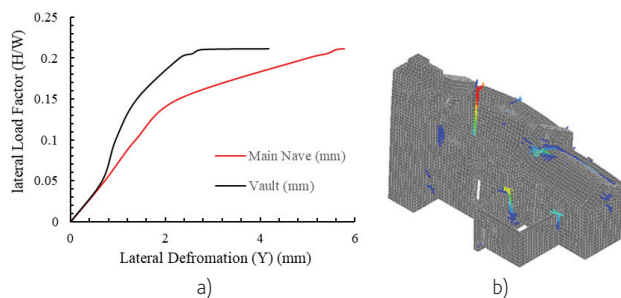


Figure 13 Pushover analysis (east-west direction): a) capacity curve; b) crack distribution

For the pushover analysis in the north-south direction, several cases of the Church's geometry were considered: without the tower, with the full tower, and with the tower at the same height as the main wall of the Church. This was done because the tower was not always have been a part of the main church and it was important to know the effect of the tower in different periods of its construction. The case with the tower at the same height as the main wall is presented for this particular case, a lateral capacity of 0.25 g was defined (Figure 14a), and at that stage, the crack distribution at the main nave is shown in Figure 14b.

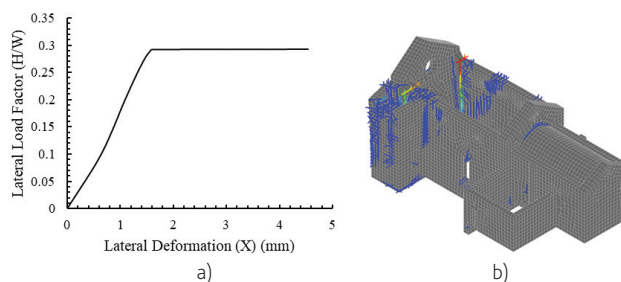


Figure 14 Pushover analysis (north-south direction): a) capacity curve; b) crack distribution

6 Conclusions

The Church of Barrô shows structural damage such as cracks and deformation and other types of deteriorations, as described. Cracks were also identified internally with means of NDT. Additionally, with the help of NDT it was possible to detect the geometrical composition of the walls and their mechanical properties to be later

utilized in the numerical model.

From the numerical nonlinear analysis, in the case of the lateral pushover in the east-west direction at 0.15 g of equivalent acceleration, it was possible to observe the same bulging observed on the side with a considerable amount of magnitude. Furthermore, with lateral pushover in the east-west direction, it was possible to obtain the damage observed on the site on the vault and northern façade. In the case of the mass-proportional pushover in the north-south direction, the model in which the tower height is the same as the church yields a considerable amount of damage like the one observed on site. Moreover, it was possible to observe the cracking pattern near the junction of the west façade and adjoining north and south façade. Given the actual code-based seismic hazard level of the area (peak ground acceleration on rock equals 0.08 g [10] and the actual conditions, the church seems to be safe from the seismic point of view.

From the pushover analyses at both the direction, it was observed that for the ground acceleration of 0.08 g, no major damage was observed except for minor cracking at the wall junctions. Moreover, these analyses were performed assuming conservative values of material properties that also contribute as a safety factor in these analyses. Apart from the localized injection of the walls aiming for its consolidation, no major structural repair works are suggested to a church standing for more than 800 years. Instead, a health monitoring system seems to be mandatory to follow the evolution of the major structural cracks.

Acknowledgments

Authors acknowledge all the technical and financial support provided within the framework of the International SAHC Masters Course (www.msc-sahc.org). Authors are very grateful for the support and assistance made available by Rota do Românico and the Northern Regional Directorate of Culture.

References

- [1] Stucchi *et al.* – “The SHARE European Earthquake Catalogue (SHEEC) 1000-1899.,” *Journal of Seismology*, no. 10.1007/s10950-012-9335-2, 2012.
- [2] ICOMOS-ISCS – “Illustrated glossary on stone deterioration patterns,” ICOMOS, 2008.
- [3] Masciotta, M.; Morais, M.; Ramos, L.; Oliveira, D.; Sanchez-Aparicio, L.; Gonzalez-Aguilera, D. – “A digital-based integrated methodology for the preventive conservation of cultural heritage: the experience of HeritageCare project,” *International Journal of Architectural Heritage*.
- [4] Borri, A.; Corradi, M.; Castori, G.; De Maria, A. – “A method for the analysis and classification of historic masonry,” *Bulletin of Earthquake Engineering*, vol. 13, no. 9, pp. 2647-2665, September 2015.
- [5] DIANA FEA BV – Displacement Method ANALyser, Release 10.1, Netherlands, 2017.
- [6] CEB-FIB – Model Code 1990: Design Code, London: Telford, 1993.
- [7] CEN, EN 1996-1-1 – Design of masonry structures, Part 1-1: General rules for reinforced and unreinforced masonry Structures, Belgium: European Committee for Standardization, 2005.
- [8] Vasconcelos, G.; Lourenço, P.B. – “Experimental characterization of the compressive behaviour,” *Mecânica Experimental*, vol. 16, pp. 61-71, 2008.
- [9] Vasconcelos, G.; Lourenço, P.B.; Alves, C. – “Experimental characterization of the tensile behaviour of granites,” *International Journal of Rock Mechanics and Mining Sciences*, vol. 45, no. 2, pp. 268-277, 2008.
- [10] NP ENV 1998-1, Eurocode 8 – Design of structures for earthquake resistance - Part 1: General rules, seismic actions and rules for buildings, Instituto Português da Qualidade, 2009.